Research Article

Photocatalytic degradation of a typical agricultural chemical: metalaxyl in water using TiO$_2$ under solar irradiation

Jahida Binte Islam[1] · **Mai Furukawa**[1] · **Ikki Tateishi**[2] · **Hideyuki Katsumata**[1] · **Satoshi Kaneco**[1,2]

Abstract

The photodegradation and mineralization of the metalaxyl [methyl *N*-(2,6-dimethyl-phenyl)-*N*-(methoxyacetyl)-alaninate], which is a popular benzenoid fungicide, was conducted in the presence of TiO$_2$ photocatalyst under solar irradiation. An initial metalaxyl concentration of 50 ppm was completely degraded in presence of TiO$_2$ after 30 min irradiation, while no degradation was observed in absence of TiO$_2$ under solar irradiation. The effect of different parameters, such as amount of TiO$_2$, initial pH, light intensity, reaction temperature and irradiation time, on the photocatalytic degradation of metalaxyl was evaluated. The drop of total organic carbon as a consequence of mineralization of metalaxyl was detected during the photocatalytic process. The kinetics of photocatalytic degradation followed a pseudo-first order law according to Langmuir–Hinshelwood model, and the rate constant was 0.105 min^{-1}. Ammonium ion and CO$_2$ were speculated as the end-products after completing degradation of metalaxyl. The five types of intermediate products were identified by GC–MS during the decomposition of metalaxyl. In order to investigate the degradation pathway of metalaxyl, the point charge and frontier electron density at each atom on the molecule were determined by using MOPAC stimulation. The degradation mechanism was proposed from the identified intermediates. The solar photocatalytic degradation method can become an effective technique for the treatment of metalaxyl-polluted water.

Keywords Metalaxyl · Photodegradation · TiO$_2$ photocatalyst · Point charge · Frontier electron density · GC–MS

1 Introduction

Metalaxyl is a fundamental benzenoid fungicide, and can be immensely applied to the plant diseases caused by Oomycete fungi [1]. Its IUPAC name is methyl *N*-(2, 6-dimethyl-phenyl)-*N*-(methoxyacetyl)-alaninate and molecular weight is 279.33 g/mol. The molecular structure of metalaxyl is shown in Fig. 1. This fungicide is very active across soil-borne and foliaceous diseases. It is continuously used in agricultural purpose because of its great tolerance for light, temperature and pH of soil [2]. Metalaxyl is frequently sprayed on plant after dilution [3]. It has long half-life in soil and it is greatly soluble in water (solubility: 8400 mg/L) which can issue a great threat of environment [4, 5]. The excessive application of metalaxyl can stimulate the contamination of soil and ground water, owing to high

✉ Jahida Binte Islam, jbislam07@gmail.com; Mai Furukawa, maif@chem.mie-u.ac.jp; Ikki Tateishi, tateishi@gecer.mie.u.ac.jp; Hideyuki Katsumata, hidek@chem.mie-u.ac.jp; Satoshi Kaneco, kaneco@chem.mie-u.ac.jp | [1]Department of Chemistry for Materials, Graduate School of Engineering, Mie University, Mie 514-8507, Japan. [2]Global Environment Center for Education and Research, Mie University, Mie 514-8507, Japan.
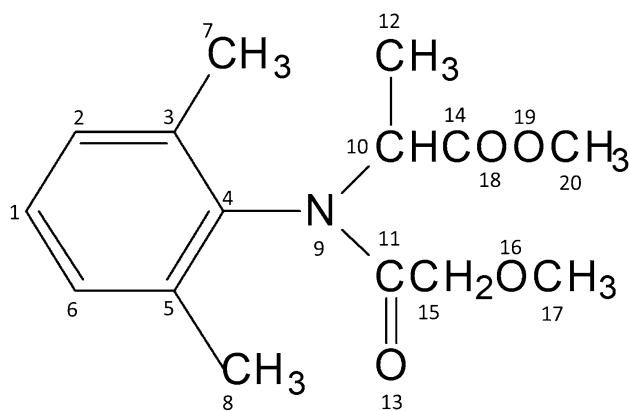
Fig. 1 Molecular structure of metalaxyl

mobility and a low soil adsorption of metalaxyl [6, 7]. In addition, metalaxyl is characterized as a stable compound in environment for the hydrolysis at normal pH values [8, 9]. These behaviors present the persistence and toxicity of metalaxyl in the environment. In addition, the minimum detection limit (MDL) of metalaxyl is tentatively 0.01 μg/L based on the report, provided by effluent characterization program [10]. Admittedly, up to 0.49 mg/L of metalaxyl, which exceeds the 0.1 mg/L EU limit, has been recorded in groundwater [11]. Therefore, the degradation of metalaxyl is essential to control its toxicity in the environment. As far, the degradation of metalaxyl has been reported by some traditional, physiochemical methods such as, microorganisms [12], Mucorales strains [13], sorption–desorption process [14], biotic process [15] and filamentous fungi [16], etc. These traditional physical or chemical methods have some major drawbacks such as costly, ineffective, time consuming and an incomplete degradation [17]. For example, Sukul et al. [14] has reported that a significant amount of metalaxyl kept tightly bound to the adsorbents after desorption cycle. Thus, desorption of 22–56% of the total amount of the retained metalaxyl was even determined. Therefore, many researchers have started to find new method for the elimination of pesticides and other pollutants from water and soil. Among the researches, the photocatalytic degradation with solar irradiation or artificial light irradiation has been considered as an effective techniques [18–20]. Photocatalytic degradation technology not only manifests a high degradation efficiency and low energy consumption with low cost, but also converts hazardous pollutant into the inorganic compound such as CO_2, water and mineral acids [21]. Conventionally, the photocatalytic method involves the migration of valence electrons to conduction band, when photocatalyst are irradiated under light having photons with more energy than bandgap of the photocatalyst [22]. So far, some significant photocatalysts, namely TiO_2, ZnO, CuO, WO_3, CdS,

Fe_2O_3, $ZnFe_2O_4$, etc., were widely studied due to favorable band gap energy to be excited under UV irradiation, low cost and suitable chemical properties [23–27]. TiO_2 and ZnO photocatalysts are highly applicable owing to their nontoxicity, wide bandgap ($E_g = \sim3.20$ eV) and high photosensitivity [28]. However, some limitations, such as the poor stability of photocatalysts except for TiO_2 in strong acidic medium, are found alongside all advantages [20, 29]. Furthermore, photocatalysts can be recycled and reused repeatedly after completing photocatalytic degradation process [30, 31]. A very few works have been reported on the photocatalytic degradation of metalaxyl under UV or solar irradiation using semiconductor based metal oxide [32, 33]. Recently, visible–light–driven photocatalytic degradation of metalaxyl with grapheme oxide/ Fe_3O_4/ZnO ternary nanohybrid was reported [10]. The solar photocatalytic treatment of wastewater is cheap, simple and environmental-friendly, compared with that using artificial lamp devices such as Hg–Xe lamp. Therefore, the solar photocatalytic degradation of metalaxyl with irradiated semiconductor photocatalyst can be considered as an effective method for degradation and mineralization of metalaxyl.

The present study demonstrates that the photocatalytic degradation of metalaxyl aqueous solution with TiO_2 photocatalyst under solar irradiation. Gas chromatography-mass spectroscopy (GC/MS) has been used to identify the intermediate products of metalaxyl. A probable reaction pathway has been drawn, depended on the generation of intermediate products. The different parameters such as catalyst dosage, pH, temperature, irradiation intensity and time have been optimized for the photocatalytic degradation of metalaxyl.

2 Experimental section

2.1 Chemicals and materials

Metalaxyl ($C_{15}H_{21}NO_4$) and hexane were purchased from FUJIFILM Wako Pure Chemical Industries Ltd., Japan. TiO_2 (P–25) was obtained from Nippon Aerosil Co. Ltd., Japan. Potassium hydrogen phthalate (C_6H_4(COOH)(COOK)), methanol (CH_3OH), dichloromethane (CH_2Cl_2), sodium carbonate (Na_2CO_3), sodium bicarbonate ($NaHCO_3$) and ammonium chloride (NH_4Cl) were purchashed from Nacalai Tesque Co. Ltd., Japan. NaOH and H_2SO_4 were used to adjust solution pH.

2.2 Photodegradation of metalaxyl

The required amount of metalaxyl powder was dissolved with ultrapure water, obtained from an ultrapure water

device (GSH-2000, Advantech Tokyo Co., Ltd.), to prepare 1000 ppm stock solution of metalaxyl. For a typical photocatalytic run, 30 mL of 50 ppm metalaxyl solution was taken into a 50 mL Pyrex reaction vessel, and 30 mg TiO$_2$ powder was added into metalaxyl solution. The pH of the solution was adjusted with 1 M NaOH and 1 M H$_2$SO$_4$. The temperature was kept constant with a water bath. The metalaxyl solution containing TiO$_2$ photocatalyst was allowed to equilibrate for 30 min in dark. Then, it was irradiated under sunlight. The suspension was continuously stirred by magnetic stirrer for the dispersion of TiO$_2$ during the treatment. The vessel wall filtered the short ultraviolet radiation ($\lambda < 300$ nm). The irradiance was measured by a UV intensity meter with sensor of 230–400 nm wavelengths (UVR-400, Iuchi Co., Osaka, Japan). The experimental set up is presented in supplementary material (Fig. S1). The 0.45 µm Advantec membrane filter was used to separate TiO$_2$ after irradiation. The high-performance liquid chromatograph equipped with a UV optical detector and ODS-3 (5 µm) column was used to evaluate the amount of metalaxyl in the aqueous solution. The elution was observed at 220 nm. The mixture of acetonitrile and water (50/50, v/v) was considered as the eluent with flow rate of 1 mL/min. The injected sample volume was 20 µL. Then, the amounts of converted NH$_4^+$ and NO$_3^-$ ions were measured by an anion ion chromatography after separating TiO$_2$ from reaction solution. The detailed analytical conditions are presented in Table S1 and S2. The degradation efficiency of metalaxyl was calculated by the following equation

$$\text{Degradation efficiency} = \left(\frac{C - C_0}{C_0} \times 100\% \right)$$

where, C and C$_0$ are the concentration of metalaxyl before and after degradation.

For total organic carbon (TOC) measurement, the mixed gas (O$_2$ + N$_2$) was passed for 30 min to remove inorganic carbon from the sample solution, and finally, the aqueous solution was subjected to determine TOC (Shimadzu TOC analyzer, TOC-V$_E$). The calibration curve TOC was prepared by preparing a solution of known concentration using potassium hydrogen phthalate.

Molecular orbital (MO) calculations were carried out at the single determinant (Hartree–Fock) level for optimization of the minimum energy obtained at the AM1 level. All semi-empirical calculations were performed in MOPAC Version 6.01 with a CAChe package (Fujitsu Co. Ltd.). The partial charge and the frontier electron density at each atom on the molecule were determined. The intermediate products were evaluated by the solid-phase extraction gas chromatography and mass spectroscopy (GC–MS). A Shimadzu gas chromatography mass spectroscopy

Table 1 Experimental conditions for GC–MS

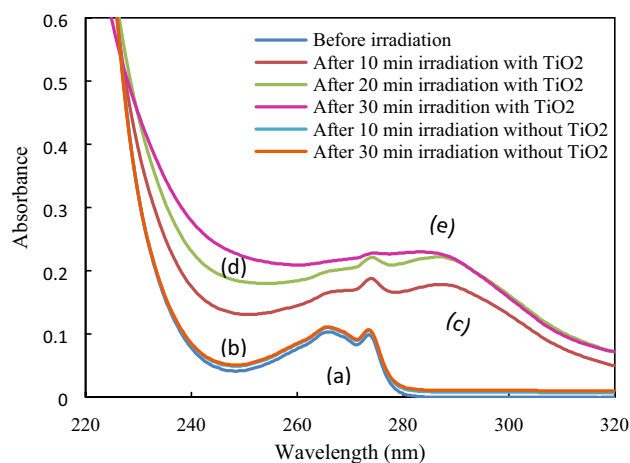|	
Capillary column	CP-Sil 8 CB (Φ: 0.25 mm × 30 m)
Column temperature program	50 °C (3 min) ⇒ up 15 °C/min ⇒ 280 °C
Injector temperature	280 °C
Interface temperature	280 °C
Carrier gas	He (99.9%), 1.5 mL/min
Ionization	Electron-impact (EI) mode
Injected volume	1 µL

Fig. 2 UV absorption spectra of metalaxyl before and after solar irradiation. Metalaxyl: 50 ppm; TiO$_2$: 20 mg; light intensity: 2.2 mW/cm^2; temperature: 20 °C and pH 6

(GCMS-QP5000, Shimadzu) equipped with a CP-Sil 8 CB capillary column was used as the chromatographic conditions of Table 1.

3 Result and discussion

3.1 UV–Vis spectral changes

The change of the UV absorption spectrum during the photocatalytic decomposition of metalaxyl by TiO$_2$ under UV irradiation has been investigated in the range of 220–320 nm by using a UV–Vis spectrophotometer. The detailed experimental conditions are presented in supplementary material (Table S3). As shown in Fig. 2, a little change in the absorption spectrum was observed after the 30 min solar irradiation without TiO$_2$ (curve b), compared to that before irradiation (curve a). Therefore, the decomposition of metalaxyl did not occur only under solar irradiation. However, the absorption spectra has been changed when TiO$_2$ was added under solar irradiation (curve c, d, e) relative to that before irradiation (curve a). Although the change in spectrum range of more than

280 nm indicated the intermediate formation of metalaxyl, the typical absorption peak (267 nm and 274 nm) for the metalaxyl decreased on using TiO_2 under solar light. Hence, this result confirms the decomposition of metalaxyl by TiO_2 under solar irradiation.

3.2 Effect of photocatalyst dosage

The effect of TiO_2 amount on the photocatalytic degradation of metalaxyl has been examined, in the range of 0–50 mg TiO_2. The results are shown in Fig. 3. The degradation efficiency was increased sharply with increasing up to 20 mg of TiO_2 and, then an almost steady result was observed in the further addition of TiO_2. Beyond a certain limit of photocatalyst amount, i.e. 20 mg of TiO_2, the reaction solution could become turbid and thusly hinder the light penetration to proceed the reaction and therefore, percentage of degradation did not increase [34, 35]. Another possible reason could be due to the constant in the portion of the irradiated surface of the photocatalyst, the obstruction of light in the dense slurry and a loss in surface area by agglomeration (particle–particle interactions) at high solid concentration [36, 37]. Therefore, 20 mg of TiO_2 was selected as the optimal amount for the subsequent experiments.

3.3 Effect of pH

The effect of pH is addressed as an important parameter during photocatalytic degradation process. The surface charge of the photocatalyst may vary with the pH value of the solution. Therefore, the effect of pH on the photodegradation of metalaxyl by TiO_2 under 10 min solar

irradiation was examined in pH range from 2 to 10. It is noteworthy to mention that the initial pH of the reaction solution was 6 without adjustment. As shown in Fig. 4, the highest 76% degradation efficiency was recorded at pH 8. The degradation efficiency was almost the same for pH 4–7. By considering the treatment cost and environmental safety, it was desirable to decompose metalaxyl near neutral pH.

The adsorption of metalaxyl onto TiO_2 surface has been measured from the stimulation of molecular partial charges (Table 2). The most negative partial charged atoms in metalaxyl are the two oxygen atoms (13O and 18O) along 9 N nitrogen atom, while the most positive partial charged atom is carbon atom (11C). The point zero charge of TiO_2 is approximately 6.5. Therefore, TiO_2 surface is predominantly positively charged below this

Fig. 4 Effect of pH on the photocatalytic degradation of metalaxyl under solar irradiation. Metalaxyl: 50 ppm; TiO_2: 20 mg; irradiation time: 10 min; light intensity: 2.2 mW/cm^2 and temperature: 20 °C

Table 2 Calculation of frontier electron density and point charge of metalaxyl

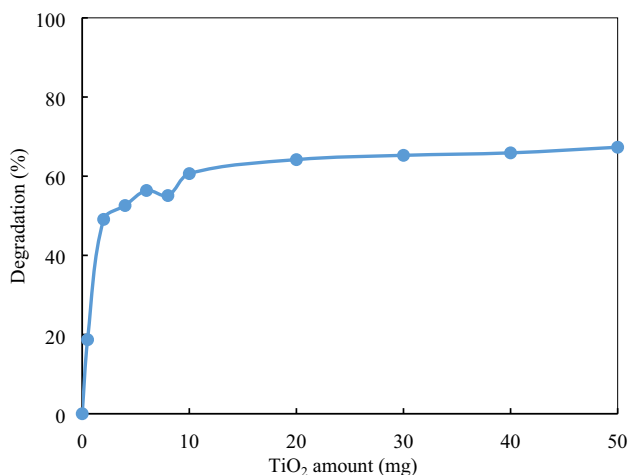| Atom	Frontier electron density	Point charge	Atom	Frontier electron density	Point charge
1C	0.233	−0.128	11C	0.043	0.319
2C	0.253	−0.15	12C	0.003	−0.231
3C	0.269	−0.06	13O	0.033	−0.384
4C	0.291	−0.037	14C	0.073	0.309
5C	0.272	−0.062	15C	0.007	−0.059
6C	0.251	−0.149	16O	0.007	−0.28
7C	0.012	−0.189	17C	0.001	−0.095
8C	0.013	−0.185	18O	0.034	−0.374
9N	0.08	−0.312	19O	0.012	−0.266
10C	0.032	0.052	20C	0.003	−0.091

Fig. 3 Effect of TiO_2 dosage on the photocatalytic degradation of metalaxyl under solar irradiation. Metalaxyl: 50 ppm; irradiation time: 10; pH 6; light intensity: 2.2 mW/cm^2 and temperature: 20 °C
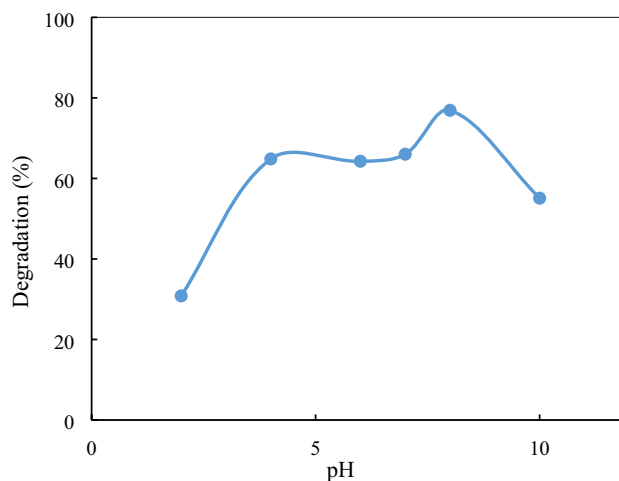
pH and negatively charged above pH 6.5 [38]. Hence, because of the electrostatic attraction, the positively charged Carbon 11C atom is readily adsorbed on the TiO_2 surface in alkaline media (pH > 6). Contrarily, the negatively charged 13O, 18O and 9 N atoms can be adsorbed on TiO_2 in acidic condition (pH < 6). Moreover, high initial pH states that more hydroxyl ions are present in solution. As a result, hydroxyl ions would be oxidized to hydroxyl radicals (·OH) by the holes forming on TiO_2 surface [39]. The photocatalytic degradation of metalaxyl can be enhanced in alkaline medium, since ·OH is the dominant oxidizing species in this photocatalytic degradation process. Therefore, pH 6 was selected for the optimal conditions to avoid the unwanted chemical treatment.

3.4 Effect of temperature

The effect of reaction temperature on the photocatalytic decomposition of metalaxyl was observed in the range of 10–60 °C. Because metalaxyl was not completely decomposed, the irradiation time was set to 10 min in order to check the influence of the reaction temperature. As shown in Fig. 5, the decomposition efficiency of metalaxyl tended to increase gradually as the reaction temperature increased, and the phenomena is comparable to other research [40]. This result concluded that a higher temperature is better for the decomposition of metalaxyl. However, the energy cost requires for raising the temperature during practical application. Therefore, the reaction temperature was set to 20 °C, because the effect of temperature was not significant in this experiment.
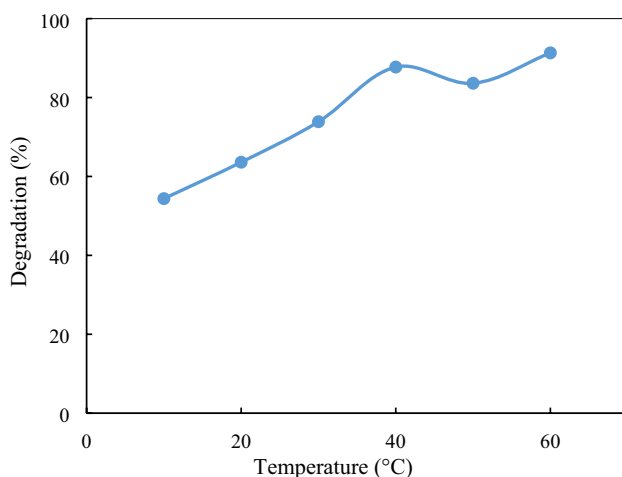
3.5 Effect of light intensity

The intensity of solar irradiation is greatly dependent on the latitude, season and time of treatment place and is related with the weather. Considering these factors, the effect of light intensity on the photo-degradation of metalaxyl with TiO_2 is essential. The photocatalytic degradation of metalaxyl was conducted under sunlight with different intensities of light in different time of sunny and cloudy days. As shown in Fig. 6, the decomposition efficiency of metalaxyl gradually increased as the light intensity increased. Generally, semiconductor based photocatalyst absorbs the light with an equal or more than band gap energy. The excitation of photocatalyst can be motivated by raising the incident light intensity [41]. Therefore, the degradation of metalaxyl is slow at low intensity of light, because of recombination of the hole-electron. On the other hand, the recombination can be prohibited by using higher light intensity [42]. Therefore, an accelerated photodegradation could be achieved with increasing the intensity of incident radiation.

3.6 Effect of light irradiation time

The effect of the light irradiation time on the photocatalytic degradation of metalaxyl with optimum experimental conditions was examined. From Fig. 7a, the degradation efficiency of metalaxyl sharply increased with increasing irradiation time in the presence of TiO_2. The degradation efficiency reached 100% with 20 mg of TiO_2 within 30 min at 20 °C. It was found from these results that the initial structure of metalaxyl was completely broken after 30 min of light irradiation. If the irradiation time increases,
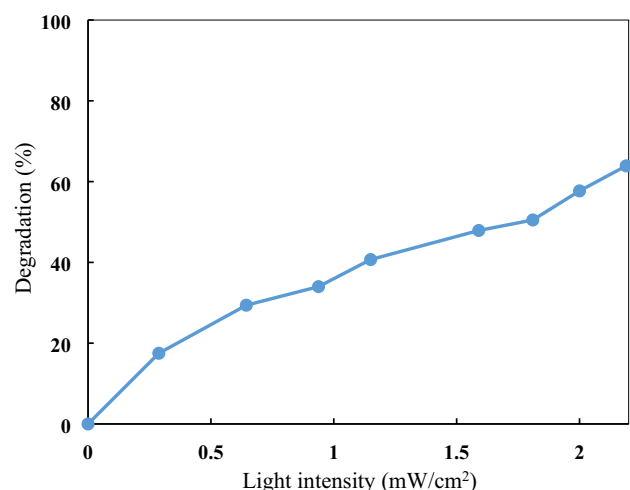

Fig. 5 Effect of temperature on the photocatalytic degradation of metalaxyl under solar irradiation. Metalaxyl: 50 ppm; TiO_2: 20 mg; irradiation time: 10 min; light intensity: 2.2 mW/cm^2 and pH 6

Fig. 6 Effect of light intensity on the photocatalytic degradation of metalaxyl under solar irradiation. Metalaxyl: 50 ppm; TiO_2: 20 mg; irradiation time: 10 min; pH 6 and temperature: 20 °C
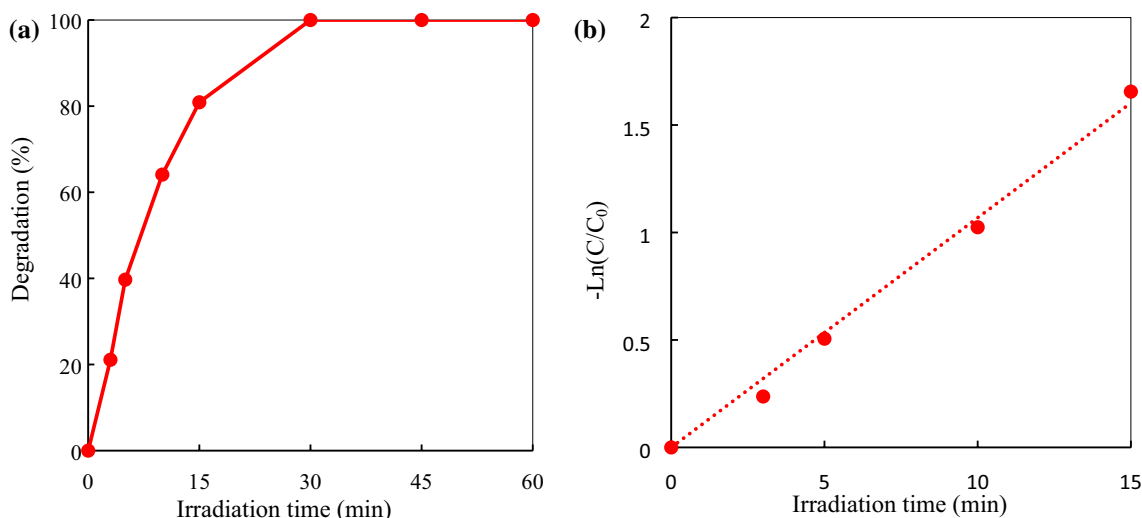
Fig. 7 **a** Effect of irradiation time on the photocatalytic degradation of metalaxyl under solar irradiation; **b** Plot of $-Ln(C/C_0)$ versus irradiation time. Metalaxyl: 50 ppm; TiO₂: 20 mg; light intensity: 2.2 mW/cm²; pH 6 and temperature: 20 °C

the interaction of metalaxyl molecule with the surface of TiO₂ will also be increased. Therefore, the photodegradation efficiency was increased eventually as shown in other research [43].

3.7 Kinetics

The kinetics of photocatalytic degradation process have been studied according to the Langmuir–Hinshelwood (L–H) model [44], and this model was motivated by Turchi and Ollis [45]. The photocatalytic degradation of metalaxyl with TiO₂ is postulated to be consistent with the Langmuir–Hinshelwood (L–H) model and expressed as Eq. 1

$$r = -\frac{dC}{dt} = \frac{kKC}{1 + KC} \qquad (1)$$

where, r is the degradation rate of the reactant, k is the rate constant, K is the adsorption co-efficient and C is the substrate concentration. When the initial concentration C_0 is very small (Eq. 1), it can be simplified to (Eq. 2), and becomes a linear expression of time t with respect to Ln(C/C_0), here, k_{app} is reaction rate constant.

$$-Ln\left(\frac{C}{C_0}\right) = kKt = k_{aap}t \qquad (2)$$

So as to confirm the speculation, $-Ln(C/C_0)$ was plotted as a function of the treatment time (irradiation time) for the photocatalytic decomposition and photolysis of metalaxyl. Because the liner relations were obtained in Fig. 7b as expected, the reduction kinetics of photodegradation of metalaxyl could follow pseudo-first-order kinetics, the fact

was consistent with the Langmuir–Hinshelwood model, resulting from the low coverage in the experimental concentration range (50 ppm). The pseudo-first-order reaction rate constants for photocatalytic decomposition of metalaxyl was 0.105 min⁻¹, and the half-life was 6.60 min. The kinetic studies confirmed that photocatalytic decomposition of metalaxyl by TiO₂ was effective because it proceeded by the photolysis reaction of metalaxyl.

3.8 Mineralization

As shown in Fig. 7, metalaxyl completely decomposes in presence of TiO₂ after 30 min of solar irradiation. Many intermediates of metalaxyl were detected in this degradation process. Therefore, it is necessary to examine the mineralization of metalaxyl. The photocatalytic mineralization of nitrogen containing organic compounds predominantly depends on the chemical nature of the organic pollutant, that is, the oxidation state and the position of nitrogen atoms in molecular chain [46, 47]. It has been reported that a complete oxidation of nitrate ions does not occur during the mineralization of organic compounds containing N. In the mineralization, ammonium ion can also be generated [48, 49]. Probably, ammonium ion, nitrate ion and CO₂ can be considered as the mineralization product of metalaxyl. A hypothesized equation is shown here for total mineralization reaction of metalaxyl solution with TiO₂ nanoparticles, assuming that the ammonium and nitrate ions were generated from nitrogen atom of metalaxyl.

$$2C_{15}H_{21}NO_4 + 37O_2 \rightarrow NO_3^- + NH_4^+ + 30CO_2 + 19H_2O \qquad (3)$$
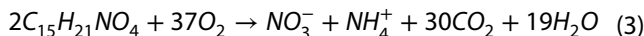
The amount of produced ammonium ion and nitrate ion from mineralization of nitrogen atom of metalaxyl, was investigated. The productions of nitrate and nitrite ions could not be confirmed by ion chromatography. The amount of produced ammonium ion was increased with the light irradiation time, and the total nitrogen yield became constant at about 86% after 6 h (Fig. 8a). It is considered that the remaining of nitrogen atoms (about 14%) may be converted into the nitrogen gas, thusly, the yield of total nitrogen was not 100%. The same type of result has been already reported in the photocatalytic degradation of other organic nitrogen compounds. Therefore, it was confirmed that the nitrogen atoms were almost mineralized under the solar irradiation. It is assumed that the ammonium ion could be generated when the intermediate products containing amino group ($-NH_2$) are mineralized.

Generally, total organic carbon (TOC) indicates the amount of organic carbon dissolved in the aqueous solution. The decrease in TOC corresponds to the mineralization of organic carbon compounds in the aqueous solution. Therefore, the change of TOC in aqueous solution was examined during the photocatalytic degradation of metalaxyl. The results are shown in Fig. 8b. The theoretical TOC value of a 50 ppm metalaxyl solution is 32.25 ppm. From Fig. 8b, TOC decreased with the light irradiation time, and reached about 10 ppm after 1.5 h. About 70% of TOC could be removed within 1.5 h of light irradiation time in the presence of TiO_2. The results indicate that the dissolved organic carbon was mineralized into CO_2 by photocatalytic decomposition. Because after 5 h of solar irradiation, about 28% of TOC remained, the relatively stable intermediates may be formed during the photocatalytic treatment.

3.9 Identification of the intermediate products of metalaxyl photocatalytic degradation under solar degradation

It was found that metalaxyl can be degraded and mineralized by the photocatalytic action of TiO_2. On the other hand, the various intermediates may be generated before the mineralization. Therefore, the intermediates from of metalaxyl was identified using a gas chromatography-mass spectrometer (GC–MS). The experimental conditions are given in supplementary information (Fig. S2). In the photocatalytic degradation, the reaction intermediates were extracted by solid phase extraction and analyzed by GC–MS. Five intermediate products has been identified by molecular ion and mass fragment peak and by comparing with GC/MS NIST library data. Based on the result obtained from GC–MS, the intermediate products are listed in Table 3. The intermediate products had more than 85% similarities for the NIST library data.

3.10 A study on the probable mechanism of photocatalytic degradation of metalaxyl with TiO_2

The photocatalytic degradation mechanism of metalaxyl is quite complex process. According to the present study and literature reports, the photocatalytic degradation mechanism of metalaxyl with TiO_2 would be represented in Scheme 1. Most of the organic pollutants can degrade under sun light irradiation in presence of suitable metal oxide-based semiconductors. The nanosized TiO_2 with the bandgap of 3.2 eV can efficiently absorb the photons with energy-greater than
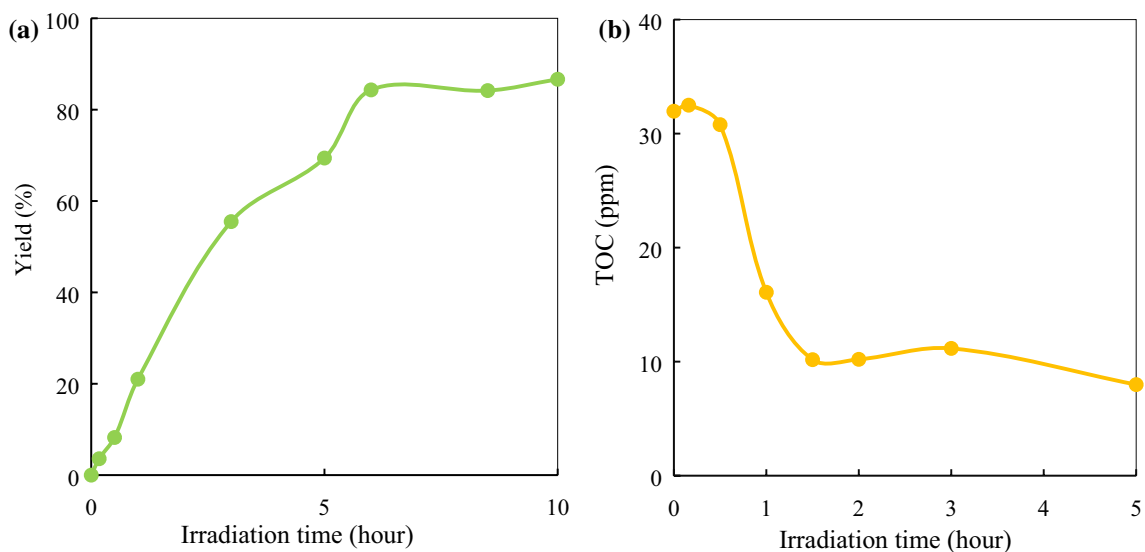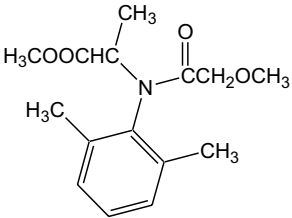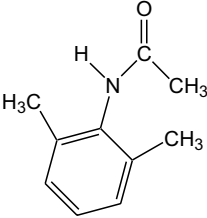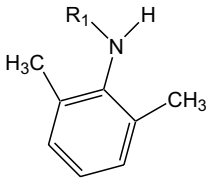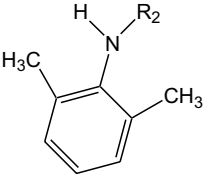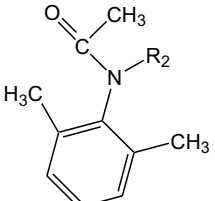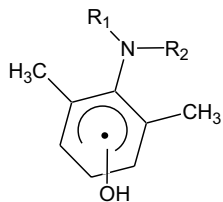

Fig. 8 a Formation of NH_4^+ ions and (b) removal of TOC during the photocatalytic degradation of metalaxyl in presence of TiO_2 under solar irradiation

Table 3 Intermediates obtained during the photodegradation of metalaxyl

Peak No.	Retention time (min)	Molecular weight (m/z)	Characteristic ions (Abundance, %)	Intermediate
1 (Metalaxyl)	16.7	279	206(100) 160(93) 146(68)	
2	12.8	163	121(100) 106(52) 163(31)	
3	13.1	207	148(100 207(14)	
4	14.1	193	148(100) 120(54) 193(50)	
5	14.6	235	120(100) 193(76) 132(52)	
6	18.5	295	250(100) 176(79) 222(61)	

Scheme 1 Probable pathways for the photocatalytic degradation of metalaxyl in presence of TiO_2 under solar irradiation
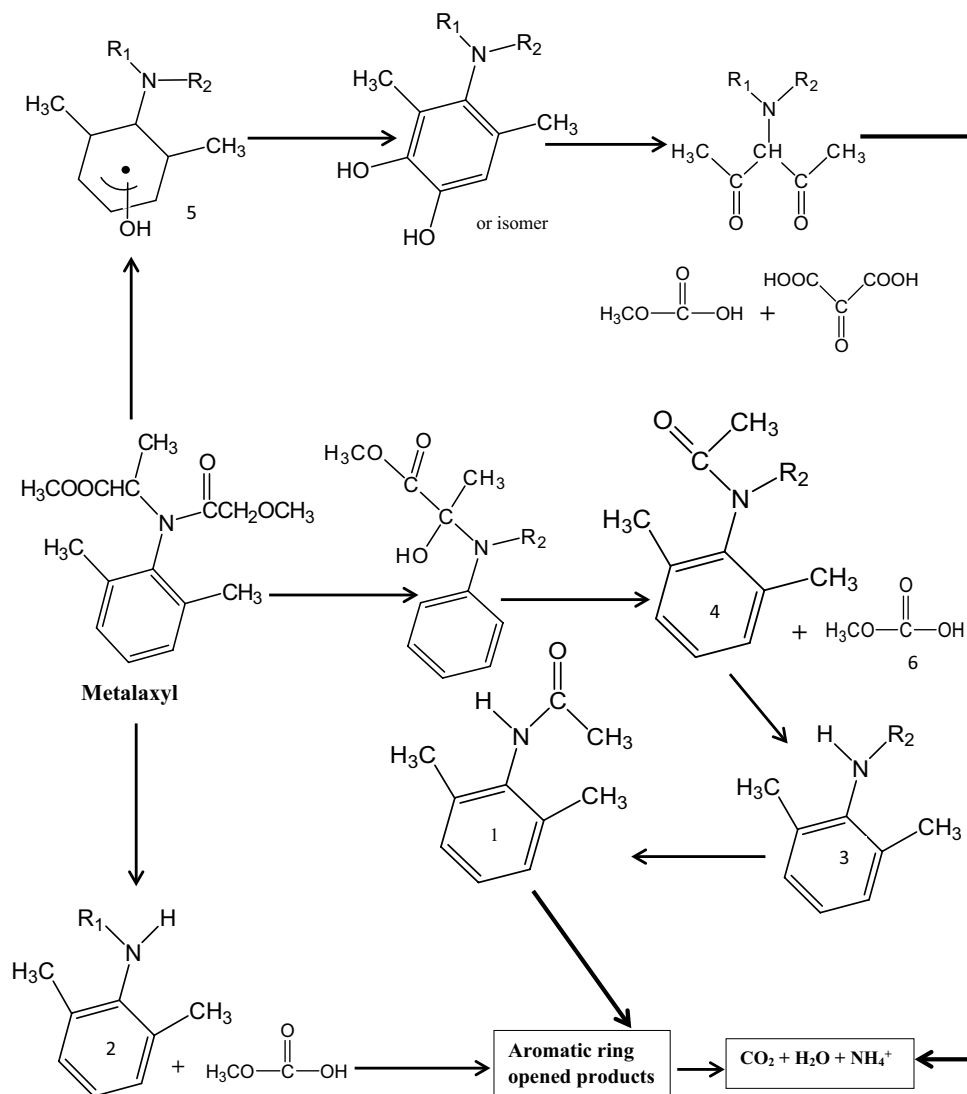
the band-gap one, and can be excited to form electrons in the conduction band (CB) and holes in the valance band (VB) under the solar irradiation [50] (Eq. 4). The oxidizing species (such as H_2O and OH^-) can be reacted with the valence band holes, h_{VB}^+, to form hydroxyl radical ($\cdot OH$) (Eq. 5), and on the other hand, the conduction band electron can be trapped by reducing species (O_2 and H_2O_2) from the reaction solution to generate mainly superoxide radicals ($\cdot O_2^-$) or hydroperoxyl radicals ($\cdot OOH$) on TiO_2 surface [51, 52] (Eqs. 5–8). These generated radicals can degrade metalaxyl into CO_2 and other products in aqueous solution (Eq. 10).

$$h_{VB}^+ + OH^- \left(or\, H_2O\right) \rightarrow \cdot OH\left(+H^+\right) \tag{5}$$

$$e_{CB}^- + O_2 \rightarrow \cdot O_2^- \tag{6}$$

$$\cdot O_2^- + H^+ \rightarrow \cdot OOH \tag{7}$$

$$2 \cdot OOH \rightarrow H_2O_2 + O_2 \tag{8}$$

$$H_2O_2 + e_{CB}^- \rightarrow \cdot OH + OH^- \tag{9}$$

$$\cdot OH(or \cdot OOH) + Metalaxyl \rightarrow\rightarrow Intermediate\ Products \rightarrow NH_4^+ + CO_2 + H_2O \tag{10}$$

$$TiO_2 + h\nu \rightarrow e_{CB}^- + h_{VB}^+ \tag{4}$$
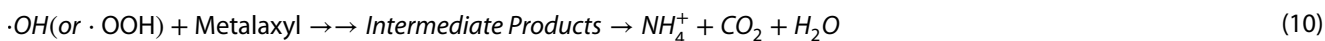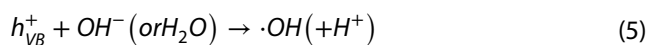
According to the MOPAC simulation (Table 2), 1C, 2C, 3C, 4C, 5C and 6C have comparatively higher frontier electron density. These sites would be attacked by neutral

·OH radicals. Especially, because of the steric hindrance, 1C, 2C and 6C could easily be attacked by ·OH radicals. Three probable degradation routes have been speculated roughly from the results of frontier electron calculations and the intermediate analysis. As a first route, hydroxyl radicals could attack the 1C, 2C or 6C of benzene ring, successively. Eventually, metalaxyl could be hydroxylated and can be converted into the intermediate 5 or its isomer. Thereafter, the benzene ring will be broken because of continuous attack of radical species. As the second route, C in alkyl group (R1) undergoes a radical attack and R1 would be hydroxylated. Then, two intermediates, namely intermediate 4 and 6, are formed. The intermediate 4 will be transformed into intermediate 3 by the attack of ·OH. Then, alkyl group (R2) of intermediate 3 is subjected to a radical attack, and intermediate 3 is converted into intermediate 1. Finally, the intermediate is mineralized into CO_2 and ammonium ion. As the third route, alkyl R2 group would be attacked by ·OH, and the intermediate 2 is generated during the photodegradation. Consequently, in every route the aromatic ring will be broken, and therefore, ammonium ion and CO_2 will be observed as final mineralization product.

The photodegradation of metalaxyl involves mainly *N*-dealkylation and demethoxylation in addition to process such as rearrangement of the *N*-acyl group to another position of the benzene and the elimination of the methoxycarbonyl group and alanine methyl ester [53]. It is difficult to identify the aliphatic compounds formed from the benzene ring opening reaction by GC–MS analysis.

4 Conclusion

The present study revealed that metalaxyl was photocatalytically degraded under sunlight. The photocatalytic action of TiO_2 can be considered as an effective and simple method for the remediation of metalaxyl contamination in water. The optimum conditions such as photocatalyst dosage, initial pH, light intensity, reaction temperature and light irradiation time was evaluated from the solar photodegradation of metalaxyl. Typically, the most optimal degradation conditions were photocatalyst dosage: 20 mg, temperature: 20 °C and pH: 6. The pseudo-first-order reaction kinetics were determined according to Langmuir–Hinshelwood model, with a degradation rate constant of 0.105 min^{-1}. The degradation of metalaxyl using TiO_2 is mainly an oxidative reaction by radical species such as hydroxyl radicals. Although metalaxyl is photo-degradable under sunlight, the addition of TiO_2 could immensely accelerate the degradation efficiency of metalaxyl. At the end of reaction, metalaxyl is almost mineralized, and ammonium ion and CO_2 were found as

final product. Hence, in the future, this research can be expected as a practical degradation and detoxification technology of metalaxyl.

Compliance with ethical standards

Conflict of interest The authors declare no conflict of interest.

References

1. Wang F, Zhu L, Wang X, Wang J, Wang J (2015) Impact of repeated applications of metalaxyl on its dissipation and microbial community in soil. Water Air Soil Pollut 226:430–444. https://doi.org/10.1007/s11270-015-2686-x
2. Sukul P (2006) Enzymatic activities and microbial biomass in soil as influenced by metalaxyl residues. Soil Biol Biochem 38:320–326. https://doi.org/10.1016/j.soilbio.2005.05.009
3. Monkiedje A, Spiteller M (2002) Sorptive behavior of the phenylamide fungicides, mefenoxam and metalaxyl, and their acid metabolite in typical Cameroonian and German soils. Chemosphere 49:659–668. https://doi.org/10.1016/S0045-6535(02)00325-9
4. Sukul P, Spiteller M (2000) Metalaxyl: persistence, degradation, metabolism, and analytical methods. Rev Environ Contam Toxicol 164:1–26
5. Wightwick AM, Bui AD, Zhang P, Rose G, Allinson M, Myers JH, Reichman SM, Menzies NW, Pettigrove V, Allinson G (2012) Environmental fate of fungicides in surface waters of a horticultural-production catchment in southeastern Australia. Arch Environ Contam Toxicol 62:380–390. https://doi.org/10.1007/s00244-011-9710-y
6. Martins MR, Santos C, Pereira P, Cruz-Morais J, Lima N (2017) Metalaxyl degradation by mucorales strains gongronella sp. and *Rhizopus oryzae*. Molecules 22(12):2225. https://doi.org/10.3390/molecules22122225
7. Sukul P, Spiteller M (2001) Persistence, fate and metabolism of [^{14}C] metalaxyl in typical Indian soils. J Agric Food Chem 49:2352–2358. https://doi.org/10.1021/jf001181r
8. Triantafyllidis V, Hela D, Patakioutas G (2013) Environmental behavior of the fungicide metalaxyl in experimental tobacco field. J Environ Sci Heal B 48(9):747–757. https://doi.org/10.1080/03601234.2013.780825
9. Massoud AH, Derbalah AS, El-SB Belal (2008) Microbial detoxification of metalaxyl in aquatic system. J Environ Sci 20(3):262–267. https://doi.org/10.1016/S1001-0742(08)60041-8
10. Dehghan S, Jafari AJ, FarzadKia M, Esrafili A, Kalantary RR (2019) Visible-light-driven photocatalytic degradation of metalaxyl by reduced graphene oxide/Fe_3O_4/ZnO ternary nanohybrid: influential factors, mechanism and toxicity bioassay. J Photochem Photobiol A 375:280–292. https://doi.org/10.1016/j.jphotochem.2019.01.024
11. Hildebrandt A, Guillamón M, Lacorte S, Tauler R, Barcelo D (2008) Impact of pesticides used in agriculture and vineyards to surface and groundwater quality (North Spain). Water Res 42:3315–3326. https://doi.org/10.1016/j.watres.2008.04.009
12. Monkiedje A, Spiteller M (2005) Degradation of metalaxyl and mefenoxam and effects on the microbiological properties of

tropical and temperate soils. Int J Environ Res Public Health 2:272–285

13. Celis R, Gámiz B, Adelino MA, Cornejo J, Hermosín MC (2015) Effect of formulation and repeated applications on the enantioselectivity of metalaxyl dissipation and leaching in soil. Pest Manag Sci 71:1572–1581. https://doi.org/10.1002/ps.3963

14. Sukul P, Lamshoft M, Zuhlke S, Spiteller M (2013) Evaluation of sorption–desorption processes for metalaxyl in natural and artificial soils. J Environ Sci Health B 48:431–441. https://doi.org/10.1080/03601234.2012.761831

15. Sukul P, Spiteller M (2001) Influence of biotic and abiotic factors on dissipating metalaxyl in soil. Chemosphere 45:941–947. https://doi.org/10.1016/S0045-6535(01)00010-8

16. Martins MR, Pereira P, Lima N, Cruz-Morais J (2013) Degradation of metalaxyl and folpet by filamentous fungi isolated from portuguese (Alentejo) vineyard soils. Arch Environ Contam Toxicol 65:67–77. https://doi.org/10.1007/s00244-013-9877-5

17. Zhang P, Sun HW, Min LJ, Ren C (2018) Biochars change the sorption and degradation of thiacloprid in soil: insights into chemical and biological mechanisms. Environ Pollut 236:158–167. https://doi.org/10.1016/j.envpol.2018.01.030

18. Farrokhi M, Yang JK, Lee SM, Shirzad-Siboni M (2013) Effect of organic matter on cyanide removal by illuminated titanium dioxide or zinc oxide nanoparticles. Iran J Environ Health Sci Eng 11:23–30. https://doi.org/10.1186/2052-336X-11-23

19. Jonidi-Jafari A, Shirzad-Siboni M, Yang JK, Naimi-Joubani M, Farrokhi M (2015) Photocatalytic degradation of diazinon with illuminated ZnO–TiO2 composite. J Taiwan Inst Chem Eng 50:100–107. https://doi.org/10.1016/j.jtice.2014.12.020

20. Ibhadon AO, Fitzpatrick P (2013) Heterogeneous photocatalysis: recent advances and applications. Catalysts 3(1):189–218. https://doi.org/10.3390/catal3010189

21. Haghighi M, Rahmani F, Dehghani R, Tehrani AM, Miranzadeh MB (2017) Photocatalytic reduction of Cr(VI) in aqueous solution over ZnO/HZSM-5 nanocomposite: optimization of ZnO loading and process conditions. Desalin Water Treat 58:168–180. https://doi.org/10.5004/dwt.2017.0145

22. Weber MF, Dignam MJ (1984) Efficiency of splitting water with semiconducting photoelectrodes. J Electrochem Soc 131:1258–1265. https://doi.org/10.1149/1.2115797S

23. Islam JB, Furukawa M, Tateshi I, Katsumata H, Kaneco S (2019) Photocatalytic reduction of hexavalent chromium with nanosized TiO2 in presence of formic acid. Chem Eng 3:33–42. https://doi.org/10.3390/chemengineering3020033

24. Farrokhi M, Hosseini SC, Yang JK, Shirzad-Siboni M (2014) Application of ZnO–Fe3O4 nanocomposite on the removal of azo dye from aqueous solutions: kinetics and equilibrium studies. Water Air Soil Pollut 225:1–12. https://doi.org/10.1007/s11270-014-2113-8

25. Mohagheghian A, Karimi SA, Yang JK, Shirzad-Siboni M (2015) Photocatalytic degradation of a textile dye by illuminated tungsten oxide nanopowder. J Adv Oxid Technol 18(1):61–68. https://doi.org/10.1515/jaots-2015-0108

26. Samad A, Furukawa M, Katsumata H, Suzuki T, Kaneco S (2016) Photocatalytic oxidation and simultaneous removal of arsenite with CuO/ZnO photocatalyst. J Photochem Photobiol A 325:97–103. https://doi.org/10.1016/j.jphotochem.2016.03.035

27. Islam JB, Furukawa M, Tateshi I, Katsumata H, Kaneco S (2020) Formic acid motivated photocatalytic reduction of Cr(VI) to Cr(III) with ZnFe2O4 nanoparticles under UV irradiation. Environ Technol. https://doi.org/10.1080/09593330.2020.1713902

28. Chu DW, Masuda Y, Ohji T, Kato K (2010) Formation and photocatalytic application of ZnO nanotubes using aqueous solution. Langmuir 26:2811–2815. https://doi.org/10.1021/la902866a

29. Siboni MS, Khataee A, Vahid B, Joo SW (2015) Synthesis, characterization and immobilization of ZnO nanosheets on scallop shell for photocatalytic degradation of an insecticide. Sci Adv 7(4):806–814. https://doi.org/10.1166/sam.2015.2163

30. Samad A, Ahsan S, Tateshi T, Furukawa M, Katsumata H, Suzuki T, Kaneco S (2018) Indirect photocatalytic reduction of arsenate to arsenite in aqueous solution with TiO2 in the presence of hole scavengers. Chin J Chem Eng 26:529–533. https://doi.org/10.1016/j.cjche.2017.05.019

31. Islam JB, Furukawa M, Tateishi I, Kawakami S, Katsumata H, Kaneco S (2019) Enhanced photocatalytic reduction of toxic Cr(VI) with Cu modified ZnO nanoparticles in presence of EDTA under UV illumination. SN Appl Sci 1:1240–1250. https://doi.org/10.1007/s42452-019-1282-x

32. Topalov A, Molnár-Gábor D, Csanádi J (1999) Photocatalytic oxidation of the fungicide metalaxyl dissolved in water over TiO2. Water Res 33(6):1371–1376. https://doi.org/10.1016/S0043-1354(98)00351-0

33. Ibrahim KM, Musleh SM, Nabeh I, Al-A Talal (2014) Heterogeneous photocatalysis of methomyl and metalaxyl using TiO2 supported over activated carbon. Res J Chem Environ 18(5):33–40

34. Coleman HM, Vimonses V, Leslie G, Amal R (2007) Degradation of 1,4-dioxane in water using TiO2 based photocatalytic and H2O2/UV processes. J Hazard Mater 146(3):496–501. https://doi.org/10.1016/j.jhazmat.2007.04.049

35. Naimi-Joubani M, Shirzad MS, Yang JK, Gholami M, Farzadkia M (2015) Photocatalytic reduction of hexavalent chromium with illuminated ZnO/TiO2 composite. J Ind Eng Chem 22:317–323. https://doi.org/10.1016/j.jiec.2014.07.025

36. Molla MAI, Furukawa M, Tateishi I, Katsumata H, Kaneco S (2019) Mineralization of Diazinon with nanosized-photocatalyst TiO2 in water under sunlight irradiation: optimization of degradation conditions and reaction pathway. Environ Technol. https://doi.org/10.1080/09593330.2019.1615129

37. Kaneco S, Rahman MA, Suzuki T, Katsumata H, Ohta K (2004) Optimization of solar photocatalytic degradation conditions of bisphenol A in water using titanium dioxide. J Photochem Photobiol 163(3):419–424. https://doi.org/10.1016/j.jphotochem.2004.01.012

38. Molla MAI, Furukawa M, Tateishi I, Katsumata H, Kaneco S (2018) Solar photocatalytic decomposition of probenazole in water with TiO2 in the presence of H2O2. Energy Source A 40:2432–2441. https://doi.org/10.1080/15567036.2018.1502840

39. Adewuyi YG (2001) Sonochemistry: environmental science and engineering applications. Ind Eng Chem Res 40:4681–4715. https://doi.org/10.1021/ie010096l

40. Sarina S, Waclawik ER, Zhu H (2013) Photocatalysis on supported gold and silver nanoparticles under ultraviolet and visible light irradiation. Green Chem 15:1814–1833. https://doi.org/10.1039/C3GC40450A

41. Lu Z, Challis JK, Wong CS (2015) Quantum yields for direct photolysis of neonicotinoid insecticides in water: implications for exposure to nontarget aquatic organisms. Environ Sci Technol Lett 2:188–192. https://doi.org/10.1021/acs.estlett.5b00136

42. Kumar A, Pandey G (2017) The photocatalytic degradation of methyl green in presence of visible light with photoactive Ni 0.10: La 0.05: TiO2 nanocomposites. IOSR-JAC 10(9):31–44. https://doi.org/10.9790/5736-1009013144

43. Herrmann JM (2005) Heterogeneous photocatalysis: state of the art and present applications. Top Catal 34:49–65. https://doi.org/10.1007/s11244-005-3788-2

44. Turchi CS, Ollis DE (1990) Photocatalytic degradation of organic water contaminants: mechanisms involving hydroxyl radical attack. J Catal 122:178–192. https://doi.org/10.1016/0021-9517(90)90269-P

45. Echavia GRM, Matzusawa F, Negishi N (2009) Photocatalytic degradation of organophosphate and phosphonoglycine pesticides using TiO$_2$ immobilized on silica gel. Chemosphere 76:595–600. https://doi.org/10.1016/j.chemosphere.2009.04.055

46. Khataee AR, Kasiri MB (2010) Photocatalytic degradation of organic dyes in the presence of nanostructured titanium dioxide: influence of the chemical structure of dyes. J Mol Catal A Chem 328:8–26. https://doi.org/10.1016/j.molcata.2010.05.023

47. Bamba D, Coulibaly M, Robert D (2017) Nitrogen-containing organic compounds: origins, toxicity and conditions of their photocatalytic mineralization over TiO$_2$. Sci Total Environ 580:1489–1504. https://doi.org/10.1016/j.scitotenv.2016.12.130

48. Carp O, Huisman CL, Reller A (2004) Photoinduced reactivity of titanium dioxide. Prog Solid State Chem 32:33–177. https://doi.org/10.1016/j.progsolidstchem.2004.08.001

49. Chong MN, Jin B, Chow CWK, Saint C (2010) Recent developments in photocatalytic water treatment technology: a review. Water Res 44:2997–3027. https://doi.org/10.1016/j.watres.2010.02.039

50. Fotiou T, Triantis T, Kaloudis T, Hiskia A (2015) Photocatalytic degradation of cylindrospermopsin under UV-A, solar and visible light using TiO$_2$. Mineralization and intermediate products. Chemosphere 119:89–94. https://doi.org/10.1016/j.chemosphere.2014.04.045

51. Zhao C, Pelaez M, Dionysiou DD, Pillai SC, Byrne JA, O'Shea KE (2014) UV and visible light activated TiO$_2$ photocatalysis of 6-hydroxymethyl uracil, a model compound for the potent cyanotoxin cylindrospermopsin. Catal Today 224:70–76. https://doi.org/10.1016/j.cattod.2013.09.042

52. Antoniou MG et al (2016) Chapter 1: photocatalytic degradation of organic contaminants in water: process optimization and degradation pathways, in photocatalysis: applications, pp 1–34. https://doi.org/10.1039/9781782627104-00001

53. Sukul P, Moza PN, Hustert K, Kettrup A (1992) Photochemistry of metalaxyl. J Agric Food Chem 40:2488–2492. https://doi.org/10.1021/jf00024a029)